# JOINT CHANNEL AND DATA ESTIMATION FOR ASYNCHRONOUS GSM USERS

*Maja Lončar, Christoph F. Mecklenbräuker, Ralf R. Müller* *

**ABSTRACT**

*In multiple-access communication systems co-channel interference can be mitigated by applying multiuser detection instead of treating the interference as additive noise [1]. In this paper we focus on downlink operation in a GSM-like TDMA network and investigate multiuser channel estimation and data symbol detection of two users that share the same physical channel in two adjacent cells. Such a scenario would allow a significant increase in spectral efficiency. We assume no synchronization between the base stations. Mobile terminals exploit multiple receive antennas. We propose a simple iterative receiver algorithm that performs joint channel and data estimation. The performance is evaluated by simulations.*

## 1. INTRODUCTION

Resource allocation strategies in cellular networks nowadays aim at meeting increasing demand for higher throughput, in terms of the number of users that can be simultaneously served. In a GSM network every cell is assigned a set of frequency bands, each of them can accommodate 8 users in different time slots. The frequency reuse factor is the result of a compromise between two opposite requirements: minimizing inter-cell interference on the one hand, and maximizing the number of supportable subscribers on the other. Adjacent cells in current systems use different sets of bands and strict power control within each cell further reduces interference level.

In this paper, we investigate the possibility of reducing the frequency reuse factor to one, i.e. we address the case when the two users that share the same physical channel belong to two neighbouring cells. A similar scenario was investigated in [2], where it was assumed that interfering base stations are synchronized and a cell radius small enough so that the signal of interest and the interfering signal arrive at the mobile receiver with a small offset (not larger than 3 symbols).

We will consider downlink mode without any synchronization between different base stations, which is the case in current GSM systems [3]. Thus, only if co-channel users belong to the same cell they will be synchronized, while in the adjacent-cell scenario they are asynchronous. For the latter case we propose an iterative receiver that performs joint channel estimation and data detection while exploiting signals from multiple receive antennas in the mobile terminal.

The article is organized as follows: in the next chapter we will introduce signal and channel model. Chapter 3 deals with the channel estimation problem. Receiver structure is presented in Chapter 4 and its performance is discussed in Chapter 5. Chapter 6 summarizes our work and gives final conclusions.

## 2. SIGNAL AND CHANNEL MODEL

The structure of the physical content of a time slot, i.e a burst, is specified by the GSM standard [4]. A 26-symbol long midamble, defined by the Training Sequence Code (TSC), is placed in the center of each burst, and it is used for estimating radio channel conditions. Guard period at the end of each burst prevents signals in consecutive time slots from overlapping. Hereinafter, we will ignore guard period (GP) and tail binary symbols (TB), and observe only $N_B = 142$ symbols of data and midamble as user's burst.

We will consider a flat fading channel that does not induce inter-symbol interference (ISI). The extension to the ISI case is straightforward. The total signal attenuation introduced by the channel is the result of several mutually independent processes [5]:

– *Path loss:* signal power decreases according to the power law of the distance between the transmitter and the receiver [6]

$$\frac{|a|^2}{{a_0}^2} = \left(\frac{r}{r_0}\right)^{-\alpha},$$

where $a$ and $a_0$ are amplitude weights at distance $r$ and reference distance $r_0$, respectively, and $\alpha$ is the path loss exponent that depends on the environment.

*) Telecommunications Research Centre Vienna (ftw.)
Tech Gate Vienna, Donau–City Str. 1/III
A–1220 Vienna, Austria
e-mail: {loncar, cfm, mueller}@ftw.at

– *Large scale fading* (*shadowing*) occurs due to large obstacles in the signal propagation path. It is a slowly varying process, modelled stochastically with log-normal distribution: $20\log(s)$ [dB] $\sim \mathcal{N}(\mu_s, \sigma_s^2)$.
– *Small scale fading* is the result of multipath propagation. The amplitude of the received faded signal is modelled as a random variable with Rayleigh distribution.

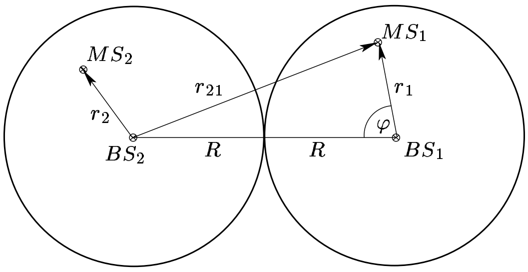


Figure 1: *Two co-channel users in adjacent cells*

The scenario when two interfering users belong to two adjacent cells is illustrated in Figure 1. The cells are modelled as circular areas of radius *R*, with the base transceiver station (BTS) in the center, and the users uniformly, independently identically distributed (i.i.d.) inside. Let $MS_1$ denote the mobile user of interest, served by the BTS $BS_1$. The interfering user $MS_2$ in served on the same channel by $BS_2$. Power control performed in the downlink will compensate the attenuation caused by shadowing and path loss between $BS_1$ and $MS_1$. However, the amplitude of the interfering signal from $BS_2$ will be received at $MS_1$ attenuated by shadowing and path loss coefficients given respectively by:

$$s = \frac{s_{21}}{s_2} \quad ; \quad p = \frac{p_{21}}{p_2} = \left(\frac{r_{21}}{r_2}\right)^{-\alpha/2}, \tag{1}$$

with the notation corresponding to Fig. 1. The baseband model of the signal received on $N_a$ antennas of $MS_1$ is

$$\boldsymbol{y}(i) = x_1(i)\,\boldsymbol{h}_1 + s\,p\,x_2(i)\,\boldsymbol{h}_2 + \boldsymbol{n} \tag{2}$$

where $\boldsymbol{y}(i)$ is $(1 \times N_a)$ row vector of the $i$-th symbol interval, $i = 1, 2, ...N_B$, $x_1(i), x_2(i) \in \{-1, +1\}$ are $i$-th transmitted symbols from $BS_1$ and $BS_2$, $\boldsymbol{n}$ is a complex white Gaussian noise vector with zero mean and variance $\sigma^2$, and $\boldsymbol{h}_1$ and $\boldsymbol{h}_2$ are $(1 \times N_a)$ channel impulse response vectors containing i.i.d. complex Gaussian coefficients for each receiving antenna. Thus, they can be viewed as unique spatial signatures characterising each user's signal space almost surely. Note that such a system with $K$ transmit antennas ($K = 2$ in our case) and $N_a$ receive antennas is equivalent to a CDMA system with $K$ users and spreading factor equal to $N_a$ [7].

Path loss and shadowing are slowly varying processes that do not change significantly over several time slots. That enables reliable estimation of coefficients $s$ and $p$, which are therefore assumed to be perfectly known to the receiver in our model. However, Rayleigh fading coefficients may change rapidly from one slot to another and therefore need to be estimated for each burst. They are considered to be invariant during one burst duration.

## 3. CHANNEL IDENTIFICATION PROBLEM

In order to enable identification and estimation of the two users' channels, different training sequences for each user are necessary requirement. Moreover, we assume that the user of interest knows the training sequence of the interferer, which makes joint channel estimation possible.

In the synchronized case bursts of the signal of interest and the interferer will overlap in time and thus their midambles will be aligned. This allows performing joint channel estimation as proposed in [2]. If synchronization is not perfect a small offset between the bursts will exist. Then the same procedure can be applied only over the overlapping segment of the two midambles. However, when the base stations are not synchronized a random offset between signals will occur. It can have an arbitrary value from 0 to burst duration, but let us assume that it is a multiple of symbol period $T_s$, known at the receiver side. Then, normalized offset values are in the range of: $N_{offset} \in \{0, 1, ..., N_B - 1\}$.

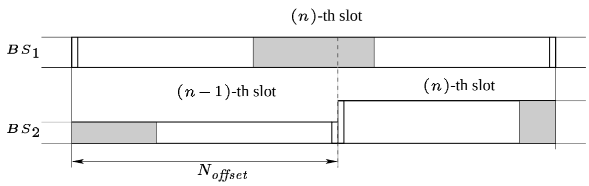


Figure 2: *Offset bursts*

Figure 2 depicts the case for $59 \leq N_{offset} \leq 84$, when the midamble of the interferer is "split" into two parts. One burst will be affected by two unequal power interfering bursts from two consecutive time slots. Since they belong to two users, they are transmitted from $BS_2$ with different powers, but they share the same channel to $MS_1$.
Collecting $N_B$ received vectors given by (2) into a $(N_B \times N_a)$ matrix $\boldsymbol{Y} = \left[\boldsymbol{y}^T(1)\ \boldsymbol{y}^T(2)\ ...\ \boldsymbol{y}^T(N_B)\right]^T$, the received burst can be written as

$$\boldsymbol{Y} = \boldsymbol{x}_1\boldsymbol{h}_1 + \tilde{\boldsymbol{x}}_2\boldsymbol{h}_2 + \boldsymbol{N}, \tag{3}$$

where $\boldsymbol{x}_1 = [x_1(1)\ x_1(2)\ ...\ x_1(N_B)]^T$ and $\tilde{\boldsymbol{x}}_2 = [s'p'\boldsymbol{x}_2(1,..,N_{offset})\ \ s''p''\boldsymbol{x}_2(N_{offset}+1,..,N_B)]^T$.
Since midambles overlap with unknown data bits, channel estimation needs to be done jointly with data detection.

## 4. RECEIVER ALGORITHM

Let $\boldsymbol{Y}_{m_1}$ and $\boldsymbol{Y}_{m_2}$ denote matrices defined according to (3), which contain the part of the received burst that corresponds to midamble $\boldsymbol{m}_1$ of user of interest and $\boldsymbol{m}_2$ of interferer, respectively. As initialization step, first channel estimates of both signals are obtained like in the single user case, regarding the other signal as noise:

$$\hat{\boldsymbol{h}}_1^{(0)} = \frac{1}{26}\,\boldsymbol{m}_1^T\,\boldsymbol{Y}_{m_1} \;\; ; \;\; \hat{\boldsymbol{h}}_2^{(0)} = \frac{1}{26}\,\boldsymbol{m}_2^T\,\boldsymbol{Y}_{m_2}. \tag{4}$$

These estimates, together with the known attenuation of the interfering signal are used to determine which signal is stronger. The iterative algorithm starts with the detection of that signal, setting the weaker channel estimate back to zero. Without loss of generality, let us assume that signal of interest (from $BS_1$) is stronger, and therefore we set $\hat{\boldsymbol{h}}_2^{(0)} = 0$. As Figure 3 indicates, in each iteration step $j = 1, \ldots M$, channel estimates are improved using the soft estimates of the data bits that overlap with midambles

$$\begin{aligned} \hat{\boldsymbol{h}}_1^{(j)} &= \frac{1}{26}\,\boldsymbol{m}_1^T \left(\boldsymbol{Y}_{m_1} - \breve{\breve{\boldsymbol{x}}}_{2\,m_1}^{(j-1)}\hat{\boldsymbol{h}}_2^{(j-1)}\right) \\ \hat{\boldsymbol{h}}_2^{(j)} &= \frac{1}{26}\,\boldsymbol{m}_2^T \left(\boldsymbol{Y}_{m_2} - \breve{\boldsymbol{x}}_{1\,m_2}^{(j)}\hat{\boldsymbol{h}}_1^{(j)}\right). \end{aligned} \tag{5}$$

The soft decision function used for obtaining intermediate symbol estimates is hyperbolic tangent, with the slope determined by signal-to-noise ratio (SNR). It can be shown that for binary signals in Gaussian noise this decision function is optimal in terms of minimizing mean square estimation error (MSE) [8], [9]. Thus, tentative decisions on data symbols in $j$-th iteration are given by:

$$\begin{aligned} \breve{\boldsymbol{x}}_1^{(j)} &= \tanh\left\{ S\hat{N}R^{(j)} \cdot \mathrm{Re}\left[\hat{\boldsymbol{h}}_1^{H\,(j)}\left(\boldsymbol{Y} - \breve{\breve{\boldsymbol{x}}}_2^{(j-1)}\hat{\boldsymbol{h}}_2^{(j-1)}\right)\right]\right\} \\ \breve{\breve{\boldsymbol{x}}}_2^{(j)} &= \tanh\left\{ S\hat{N}R^{(j)} \cdot \mathrm{Re}\left[\hat{\boldsymbol{h}}_2^{H\,(j)}\left(\boldsymbol{Y} - \breve{\boldsymbol{x}}_1^{(j)}\hat{\boldsymbol{h}}_1^{(j)}\right)\right]\right\}. \end{aligned} \tag{6}$$

The estimates of SNR are updated in each iteration as

$$S\hat{N}R^{(j)} = \frac{\parallel \hat{\boldsymbol{h}}_1^{(j)} \parallel^2}{\hat{\sigma}^2} \tag{7}$$

$$\hat{\sigma}^2 = \frac{1}{N_a}\mathrm{trace}\{\hat{\boldsymbol{P}}_{\mathcal{H}}^{\perp}\,\hat{\boldsymbol{C}}_y\}, \tag{8}$$

where $\boldsymbol{C}_y$ is $(N_a \times N_a)$ signal covariance matrix and $\boldsymbol{P}_{\mathcal{H}}^{\perp}$ is a projection matrix associated with the noise subspace. Recalling that we defined $\boldsymbol{y}$, $\boldsymbol{h}_1$, and $\boldsymbol{h}_2$ in (2) as row vectors and defining $\boldsymbol{H} = \left[\boldsymbol{h}_1^T \; \boldsymbol{h}_2^T\right]$, these matrices are given by

$$\boldsymbol{C}_y = \mathrm{E}\left\{(\boldsymbol{y}^T)(\boldsymbol{y}^T)^H\right\} = \boldsymbol{H}\boldsymbol{H}^H + \sigma^2\boldsymbol{I} \tag{9}$$

$$\boldsymbol{P}_{\mathcal{H}}^{\perp} = \boldsymbol{I} - \boldsymbol{H}(\boldsymbol{H}^H\boldsymbol{H})^{-1}\boldsymbol{H}^H \tag{10}$$

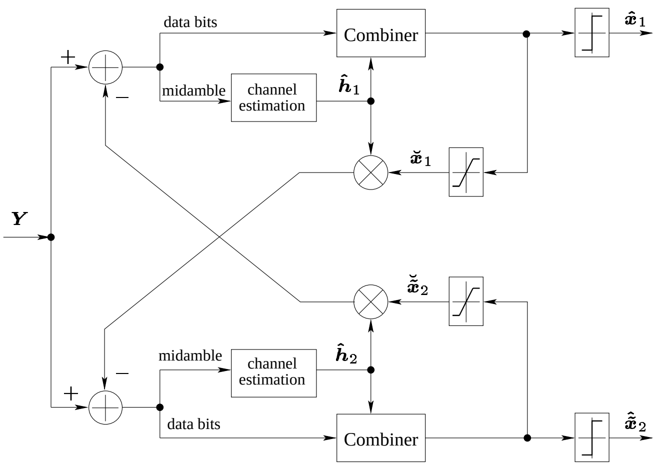


Figure 3: *Block diagram of iterative receiver*

The estimated matrices are obtained in the following way:

$$\hat{\boldsymbol{C}}_y = \frac{1}{N_B}\sum_{i=1}^{N_B}(\boldsymbol{y}_i^T)(\boldsymbol{y}_i^T)^H \quad (11)$$

$$\hat{\boldsymbol{P}}_{\mathcal{H}}^{\perp} = \boldsymbol{I} - \hat{\boldsymbol{P}}_{\mathcal{H}} = \boldsymbol{I} - \boldsymbol{Q}^H\boldsymbol{Q}, \quad (12)$$

where $\boldsymbol{Q} = \mathrm{orth}(\hat{\boldsymbol{H}})$ spans the same estimated signal subspace $\hat{\mathcal{H}}$ as $\hat{\boldsymbol{H}}$, but has orthogonal columns.

The iterative process converges rapidly. Simulations show that after $M = 3$ iterations channel estimates reach steady state, thus allowing to stop the iterations with final data symbol estimates. They are obtained by applying the hard decision rule

$$\hat{\boldsymbol{x}}_1 = \mathrm{sign}\left\{\mathrm{Re}\left[\hat{\boldsymbol{h}}_1^{H(M)}\left(\boldsymbol{Y} - \breve{\boldsymbol{x}}_2^{(M)}\hat{\boldsymbol{h}}_2^{(M)}\right)\right]\right\}$$

$$\hat{\boldsymbol{x}}_2 = \mathrm{sign}\left\{\mathrm{Re}\left[\hat{\boldsymbol{h}}_2^{H(M)}\left(\boldsymbol{Y} - \breve{\boldsymbol{x}}_1^{(M)}\hat{\boldsymbol{h}}_1^{(M)}\right)\right]\right\}.$$

## 5. PERFORMANCE EVALUATION

As a performance measure of the receiver, we observe the bit error rate (BER) as a function of mean signal-to-noise ratio (SNR), which is defined as $SNR = \overline{E_s}/N_0$, where $\overline{E_s}$ is mean energy per symbol and $N_0$ is one-sided power spectral density of white noise.

As typical values for modelling urban and suburban environment [10], path loss exponent is set to $\alpha = 4$ and shadowing attenuation weights in (1) have the same standard deviation $\sigma_{21} = \sigma_2 = 10$ dB. These values lead to huge variations of interference power. Averaged over all possible path loss values (for all possible relative positions of the mobile users) signal to interference (SIR) level amounts to $-6$ dB. In the performed simulations it was assumed that the positions of the users change from one burst to another, thus leading to independent, different instantaneous interference levels. Because of unbalanced interference levels receiver's performance is strongly dependent on the relative offset between the signals arriving from the serving and the interfering base station. Figure 4 shows BER curves for three extreme cases of offset. Obviously, for high values of offset performance degrades significantly for higher SNRs where interference has dominant influence. This behaviour is depicted by Figure 5 where, due to symmetry, relative offset can be defined as: $N_{rel} = (N_{offset} - \frac{1}{2}N_B) \in \{-71, ..., 0, ..., 70\}$.

For higher SNR (lower curve in Figure 5), the receiver is more sensitive to channel estimation errors. Both curves show that for small relative offsets, when almost the whole burst is affected by the same level of interference, the receiver is able to mitigate this interference throughout iterations. In the light of shown results, it is reasonable to require only a coarse synchronization between the two base stations. In that case the algorithm shows good performance even though the receiver does not exploit knowledge of $26 - |N_{rel}|$ overlapping bits of midambles, as proposed in [2].

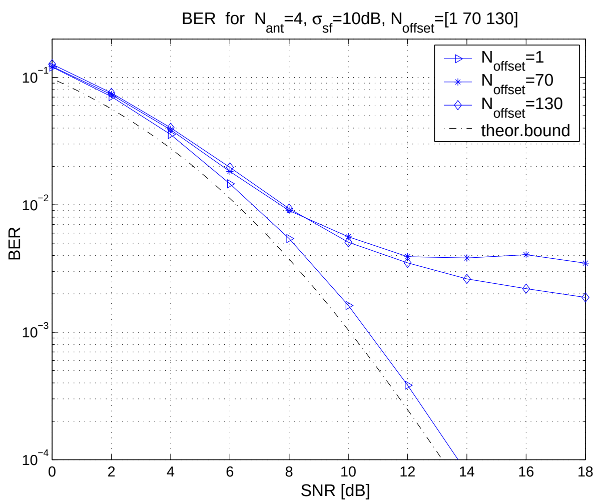


Figure 4: *BER for 3 different offset values*

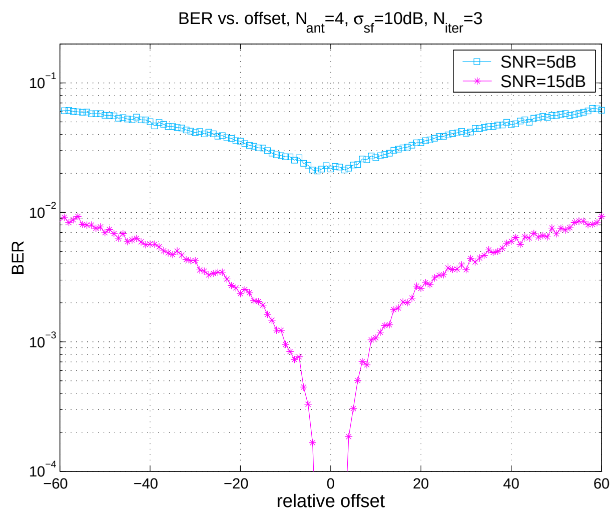


Figure 5: *BER performance versus relative offset*

Figure 6 shows the performance improvement during the iterative process. One iteration corresponds to performing only spatial matched filtering, based on the estimated channel given by (4). By second iteration performance is improved, especially in higher SNR region. The lower bound on BER of the receiver is given by the analytical result for probability of error for binary symbols in a Rayleigh fading channel, with $L$ statistically independent diversity branches. A closed-form solution for such a case is given by [11]

$$P_\epsilon = \left(\frac{1}{2}(1-\mu)\right)^L \sum_{k=0}^{L-1} \left[\binom{L-1+k}{k}\left(\frac{1}{2}(1+\mu)\right)^k\right], \tag{13}$$

where $L$ in our case equals to the number of antennas $N_a$, and $\mu$ is the function of the average SNR per channel, defined as:

$$\mu = \sqrt{\frac{SNR/N_a}{1+SNR/N_a}}.$$

Note that expression (13) assumes perfect knowledge of the channel at the receiver side and completely orthogonal users' signatures. For small values of offset receiver approaches this bound after $M = 3$ iterations, as shown in Figure 6. A performance gap of less than 1 dB is due to non-ideal channel estimation and presence of variable-power shadowed interference.

Finally, Figure 7 shows the diversity gain for different number of receive antennas, in case of small offset. As the number of antennas grows larger the BER is closer to the theoretical bound given by (13) for corresponding number of branches $L$.

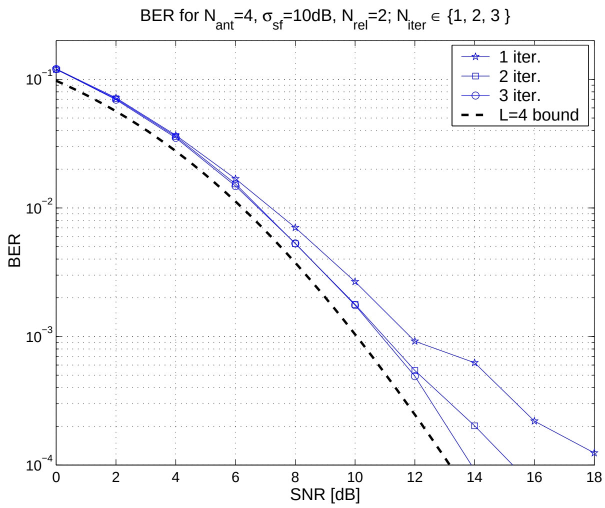


Figure 6: *Influence of number of iterations*

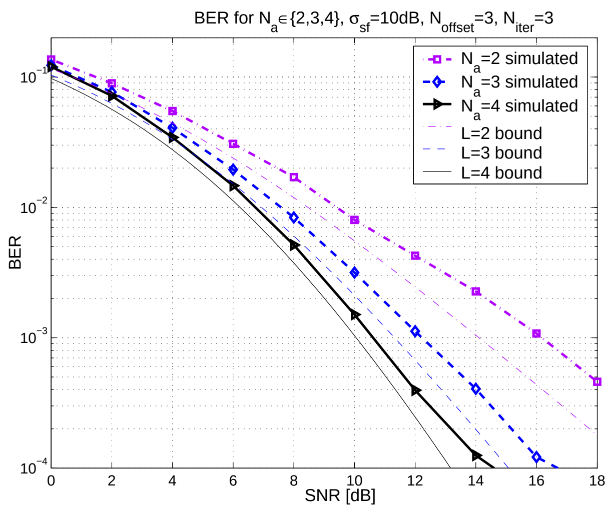


Figure 7: *BER for variable number of antennas*

## 6. CONCLUSIONS

We have investigated application of multiuser detection on two asynchronous, power imbalanced co-channel users in a GSM-like system. For a general case of an arbitrary relative offset a low-complexity iterative receiver structure is proposed, which performs joint channel estimation and data detection. For updating channel estimates in the iterative process soft decisions on data symbols are used as feedback information. The iterative process reaches steady state very quickly (after 3 iterations). Performance shows strong dependency on the relative offset. For small values of offset BER closely follows the lower bound of the single-user case in a Rayleigh-fading channel with independent receive diversity branches. The simplified receiver can be extended to handle inter-symbol interference as well as more than one interfering user.


## 7. ACKNOWLEDGMENTS

The authors would like to thank Laura Cottatellucci (ftw.), Per Ödling (Lund Institute of Technology, Sweden) and Thomas Magesacher (ftw.) for their valuable comments and support.

## 8. REFERENCES


[1] S. Verdú, *Mulituser Detection*, New York, 1998.

[2] H. Trigui and D. Slock, "Training sequence based mulituser channel identification for cochannel interference cancellation in GSM," in *Proceedings of 2nd IEEE Workshop on Signal Processing Advances in Wireless Communications, SPAWC '99*, 1999, pp. 102–105.

[3] T.S. Rappaport, *Wireless Communications - Principles & Practice*, Prentice Hall, Upper Saddle River, New Jersey, 1996.

[4] "Digital cellular telecommunications system (phase 2+); multiplexing and multiple access on the radio path, GSM 05.02 version 8.5.0 release 1999," European Standard (Telecommunications Series), Draft ETSI EN 300 908 V8.5.0, July 2000.

[5] W.C.Y. Lee, *Mobile Communications Engineering*, McGraw-Hill, New York, 1982.

[6] T.S. Rappaport (Ed.), *Cellular Radio & Personal Communications*, vol. 2: Advanced Selected Readings, IEEE, Piscataway (NJ), 1996.

[7] S.V. Hanly and D.N.C. Tse, "Resource pooling and effective bandwidths in CDMA networks with multiuser receivers and spatial diversity," *IEEE Trans. Inf. Theor.*, vol. 47, no. 4, pp. 1328–1351, May 2001.

[8] R.R. Müller and J.B. Huber, "Iterated soft decision interference cancellation for CDMA," in *Broadband Wireless Communications*, Luise and Papolin, Eds., pp. 110–115. Springer, London, UK, 1998.

[9] Sgraja C., Teich W., Engelhart A., and Lindner J., "Multiuser/multisubchannel detection based on recurrent neural network structures for linear modulation schemes with general complex-valued symbol alphabet," in *Proceedings of COST 262 Workshop on Multiuser Detection in Spread Spectrum Communications*, Schloss Reisenburg, Ulm, Germany, Jan. 2001, pp. 45–52.

[10] Members of SMG2, "Selection procedures for the choice of radio transmission technologies of the universal mobile telecommunications system UMTS (UMTS 30.03)," Tech. Rep. ETSI TR 101 112 version 3.2.0, ETSI SMG2, Apr. 1998.

[11] J. Proakis, *Digital Communications*, McGraw-Hill, New York, 2000.